

Derivation of Phase Field Crystals by Coarse-Graining in Time

P. F. Tupper¹ and Martin Grant²

¹*Department of Mathematics and Statistics, McGill University, Canada.*

²*Department of Physics, McGill University, Canada.*

(Dated: March 3, 2019)

Phase field crystals (PFC) are a tool for simulating materials at the atomic level. They combine the small length-scale resolution of molecular dynamics (MD) with the ability to simulate dynamics on mesoscopic time scales. We show how PFC can be derived by applying coarse-graining in time to the microscopic density field of molecular dynamics simulations. The correct free energy for the phase field is taken from the classical density functional theory of inhomogeneous liquids. As an example, we show how to derive the PFC free energy for Weber and Stillinger's two-dimensional square crystal potential which models a system of proteins suspended in a membrane.

PACS numbers: 05.70.Ln,64.70.Dv,61.50.Ah

Phase field crystals (PFC) were introduced in [1] as a tool for performing long-time simulation of materials at the microscopic scale. The approach is an example of the *phase field* approach to non-equilibrium modeling and simulation. The system of interest is represented by a field corresponding to the atomic density of the material. Its dynamics are simulated dissipatively according to free energy minimization with additional noise. The advantage of PFC over other phase field models is its ability to naturally resolve microscopic structure: the PFC field corresponding to a solid in equilibrium has a periodic structure matching that of the crystal structure of the material. The advantage of PFC over molecular dynamics (MD) is that fast degrees of freedom are not present in the model and this allows efficient simulation over mesoscopic time scales. The PFC approach can model elastic and plastic deformation of crystals as well as the liquid-solid transition [2] and diffusion of defects [3].

Previous work [2] demonstrated how phase field crystals could be constructed that matched the first peak in the structure factor of a two-dimensional hexagonal crystal material and demonstrated their use for the simulation of a variety of non-equilibrium phenomenon. Here we will accomplish two things: (i) show that phase-field crystals can be interpreted as the result of applying coarse-graining in time to microscopic molecular dynamics (ii) show how to generalize phase-field crystals in order to model different materials and match more than the first peak in the structure factor. The system we will use as an example for this is Weber and Stillinger's [4] two-dimensional square-crystal forming system. This system was originally proposed as a model of various systems where square two-dimensional crystals occur, including proteins suspended in a membrane and planar levels in colloidal suspensions. We will show that we can obtain a PFC free energy that matches arbitrarily many peaks of the structure factor of the time-coarsened microscopic density for this potential.

We consider a system of N particles in the plane each with mass m and with positions r_i and momenta p_i , $i =$

$1, \dots, N$. The energy of the system is given by

$$H_N = \sum_{i=1}^N \frac{p_i^2}{2m} + V(r_1, \dots, r_N). \quad (1)$$

The V used by Weber and Stillinger [4] contains both two-body and three-body terms:

$$V(r_1, \dots, r_N) = \sum_{i \neq j} v^{(2)}(|r_i - r_j|) + \lambda \sum_{i,j,k} v^{(3)}(r_i, r_j, r_k).$$

The pair potential is given by

$$v^{(2)}(r) = \begin{cases} A(r^{-12} - r^{-5}) \exp[(r - a)^{-1}], & 0 < r < a \\ 0, & r \geq a, \end{cases}$$

where $A = 6.767441$, $a = 2.46491832$. The three-body term is given by

$$v^{(3)}(r_i, r_j, r_k) = h(r_{ij}, r_{jk}, \theta_i) + h(r_{ji}, r_{jk}, \theta_j) + h(r_{ki}, r_{kj}, \theta_k),$$

where $r_{ij} = |r_i - r_j|$ and θ_i is the angle between $r_j - r_i$ and $r_k - r_i$. The function h is

$$h(r, s, \theta) = \exp[(r - a_3)^{-1} + (s - a_3)^{-1}] \sin^2(2\theta),$$

when $r, s < a_3$, and is zero otherwise. Weber and Stillinger choose $a_3 = 1.8$ and $\lambda = 5$. Without the three-body terms the potential is qualitatively the same as the Lennard-Jones potential, and the system has a hexagonal crystal phase like that modeled by the PFC in [2, 3]. The addition of the three-body term makes hexagonal structure unfavourable and the crystal phase has square symmetry [4]. The dynamics of the system were simulated using molecular dynamics.

The microscopic density field is given by $\rho_m(r, t) = \sum_{i=1}^N \delta(r - r_i(t))$, where $r_i(t)$ is the position of the i th particle at time t . We consider the density coarse-grained in time:

$$\rho(r) = \frac{1}{\tau} \int_0^\tau dt \rho_m(r) \quad (2)$$

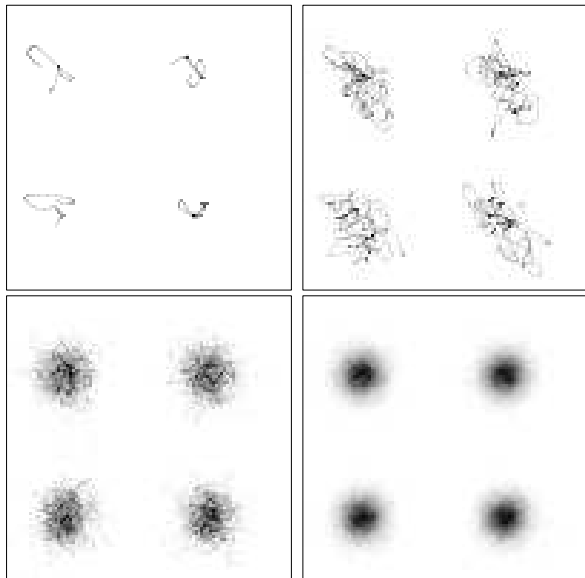


FIG. 1: Grey-scale plot of time-averaged density of portion of Weber–Stillinger MD system for reduced temperature 0.6, reduced density 0.77277. The time intervals for averaging are 1, 10, 100, 1000 time units.

If the original system is in the liquid phase, for large τ , ρ will be equal to a constant plus small, spatially homogenous, fluctuations. If the original system is in the solid phase, ρ will have a steady periodic form for large τ corresponding to the structure of the crystal. Figure 1 shows density plots of ρ of a system in solid phase for four different coarse-graining times τ . As τ is increased fluctuations about equilibrium become smaller and occur over a smaller time scale.

Our goal is to obtain a model for the dynamics of this coarse-grained density field for large but finite τ . The form of the model we choose is as follows. We hypothesize the existence of a free energy \mathcal{F} such that the dynamics of the time-coarsened density ρ is given by

$$\frac{\partial \rho(r)}{\partial t} = \Gamma \vec{\nabla} \cdot \left(\rho \vec{\nabla} \frac{\delta \mathcal{F}}{\delta \rho(r)} \right) + \vec{\nabla} \cdot \left(\sqrt{2\sigma^2 \Gamma} \sqrt{\rho} \vec{\eta}(r, t) \right), \quad (3)$$

where $\eta(r, t)$ is a mean zero noise field with

$$\langle \eta_i(r, t) \eta_j(r', t') \rangle = \sigma^2 \delta_{ij} \delta(r - r') \delta(t - t').$$

This yields dynamics in which mass is conserved. We will also consider

$$\frac{\partial \rho(r)}{\partial t} = -\Gamma \rho \frac{\delta \mathcal{F}}{\delta \rho(r)} + \Gamma \sigma^2 + \sqrt{2\sigma^2 \Gamma} \sqrt{\rho} \xi(r, t) \quad (4)$$

which corresponds to constant chemical potential. Here

$$\langle \xi(r, t) \xi(r', t') \rangle = \delta(r - r') \delta(t - t').$$

The $\Gamma \sigma^2$ term does not represent an external force but is a consequence of using multiplicative noise. It is necessary for the dynamics to satisfy detailed balance, as can

be checked with the Fokker-Planck equation. The $\sqrt{\rho}$ multiplying the noise term is motivated by dynamic density functional theory [5]. In both cases the noise should be interpreted in the Ito rather than the Stratonovich sense.

Both of these dynamics yield an equilibrium distribution for ρ proportional to $\exp(-\mathcal{F}(\rho)/\sigma^2)$. The non-conserved dynamics has the same equilibrium properties as the conserved dynamics and can be simulated numerically more efficiently. We will show that for suitably chosen \mathcal{F} and σ the dynamics of (4) matches that of the time-averaged microscopic density ρ , at a given temperature, density, and coarse-graining time τ .

The motivation for the particular free energy functional \mathcal{F} we use comes from classical density functional theory [6, 7]. The goal of Ramakrishnan and Yussouf's density functional theory is to estimate a free energy \mathcal{F} for which the infinite-time averaged density $\rho = \rho_\infty = \langle \rho_m \rangle$ is the minimal. They derive this free energy formally by integrating the partition function; the calculation can only be completed in the case of the ideal gas. To obtain usable approximations [6] postulate that ρ has a free energy $\mathcal{F}(\rho) = \mathcal{F}_{id}(\rho) + \mathcal{F}_{ex}(\rho)$ where \mathcal{F}_{id} is the ideal gas free energy and \mathcal{F}_{ex} is a functional Taylor series expansion in ρ about the uniform liquid state density. Typically, only two terms in the expansion are taken for most applications [8].

Our goal is somewhat different than that of density functional theory; we are interested in densities averaged over finite times τ , rather than infinite times. This allows us to model non-equilibrium phenomena. We start with free energies of density functional theory form and then add noise to account for our merely finite length of time-coarsening interval τ . Moreover, rather than deriving coefficients in the free energy from liquid state equilibrium correlation functions, we choose coefficients that will be easy to compute, give the correct qualitative behaviour and have parameters that can then be tuned to match MD.

Our free energy is of the form

$$\begin{aligned} \mathcal{F}(\rho) = & \int dr T \rho(r) (\log(\rho) - 1) - \int dr \rho(r) \mu \\ & + \frac{k_A}{2} \iint dr_1 dr_2 C_2(r_1, r_2) \rho(r_1) \rho(r_2) \\ & + \frac{k_B}{3} \iiint dr_1 dr_2 dr_3 C_3(r_1, r_2, r_3) \rho(r_1) \rho(r_2) \rho(r_3) \end{aligned}$$

The last cubic term is necessary to obtain a square crystal structure and is analogous to the three-body potential term in [4]. The variable T corresponds to temperature. The kernel C_2 is symmetric and translationally invariant and defined by $C_2(r_1, r_2) = c(r_1 - r_2)$ where

$$c(r) = \frac{1}{2} \arctan \left(\frac{20(r/r_0 - 1)}{2\pi} - 1 \right).$$

For ease of computation, this function is then truncated at radius $3r_0$ and shifted down to be continuous. We fix $r_0 = 6$ and $k_A = 1$. The kernel C_3 is given by

$$C_3(r_1, r_2, r_3) = U(r_{12}, r_{13}, \theta_{123}) + U(r_{21}, r_{23}, \theta_{213}) \\ + U(r_{31}, r_{32}, \theta_{312})$$

where $r_{ij} = |r_j - r_i|$ and θ_{ijk} is the angle between $r_j - r_i$ and $r_k - r_i$. We let

$$U(r_{12}, r_{23}, \theta) = H(r_{12})H(r_{23}) \sin^2(\theta)$$

where

$$H(r) = \exp[(r - r_{max})^{-1} + (r_{min} - r)^{-1}],$$

for $r_{min} < r < r_{max}$ and $H(r) = 0$ otherwise. We fix $r_{min} = 6$, $r_{max} = 10$ and $k_B = 0.05$.

With this choice of \mathcal{F} the equations for non-conserved dynamics (4) are then

$$\frac{\partial \rho}{\partial t} = -\Gamma \rho [T \log \rho - \mu + k_A \mathcal{C} \rho + k_B \mathcal{D}(\rho, \rho)] \\ + \Gamma \sigma^2 + \sigma \sqrt{2\Gamma \rho} \xi,$$

where $\mathcal{C} \rho(r_1) = \int dr_2 c(r_1 - r_2) \rho(r_2)$ and

$$\mathcal{D}(\rho, \rho)(r_1) = \iint dr_2 dr_3 C_3(r_1, r_2, r_3) \rho(r_2) \rho(r_3).$$

Here ξ is noise white in space and time.

To numerically simulate the dynamics ρ is discretized on a rectangular grid. In the units we use, the distance between two adjacent points on the grid is 1 unit. All integrals are evaluated by straightforward summation on the grid. The equation are integrated in time using the explicit Euler method, typically with a time step of length $\Delta t = 0.01$.

For particular values of the parameter μ and without noise ($\sigma = 0$) the field ρ has two possible equilibria selected depending on T . For large T the log term dominates and the stable equilibrium is a constant ρ corresponding to a liquid state. As T is decreased, this state becomes unstable and the system has a periodic free energy minimum resembling the fourth plot in Figure 1. With the parameters described here the distance between two adjacent bumps in the periodic phase is approximately 8.5 units.

Figure 2 shows a non-equilibrium simulation of the system with non-conserved dynamics. With $\mu = 10$, $T = 2.2$, $\sigma = 0$ the system was started in the equilibrium crystal state except for one one patch consisting of square of 25 particle bumps which is rotated 45° . The system was integrated in time until close to the uniform solid configuration equilibrium. In grey-scale we show density plots of the system for four representative times.

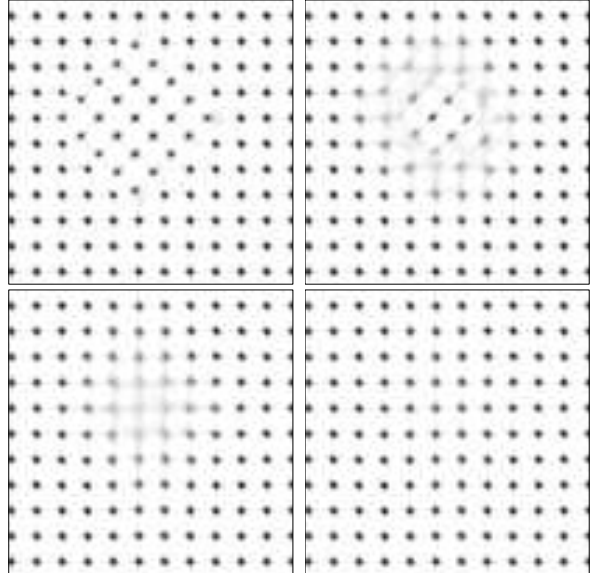


FIG. 2: Grey-scale plot of ρ on a portion of the computational domain during simulation with non-conserved dynamics. Plots shown at 0, 33, 66, 99 time units.

We now compare results numerically obtained using this free energy with those of time-averaged molecular dynamics. For a wide range of temperatures, densities, and time-coarsening times of the MD system, we can choose T , μ and σ for the PFC to obtain good agreement.

Figure 3 shows the structure factor for a time-averaged MD simulation together with the structure factor for an equilibrium PFC configuration where parameters have been chosen to obtain the best fit. The MD structure factor was taken from a 400 particle system in a perfect square crystal of density 0.77277 (leading to the minimum energy for the ground state) and reduced temperature 0.55. The PFC was obtained from a non-conserved dynamics run with $\mu = 10$, $T = 0.8$, $\sigma = 0.02$. All peaks in the MD structure factor in the range shown are present in the PFC, and the amplitudes match quite closely. Only two parameters were adjusted to fit the first two peaks; the others peaks matched without further tuning.

Using MD, Weber and Stillinger observe a first order melting transition for the square crystal system, and found no evidence for a two-stage melting process [4]. We perform an analogous experiment using our PFC model of the system. As in [4], we examine the liquid-solid transition by starting the system in a perfect square crystal and increasing the temperature (in our case, the parameter T) slowly. We used the non-conserved dynamics with $\mu = 30$, and $\sigma = 0, 0.01, 0.02, 0.04$. In Figure 4 we show the negative derivative of mean density $\bar{\rho}$ with respect to T as a function of T . Our results are consistent with those of Weber and Stillinger for the same transition and

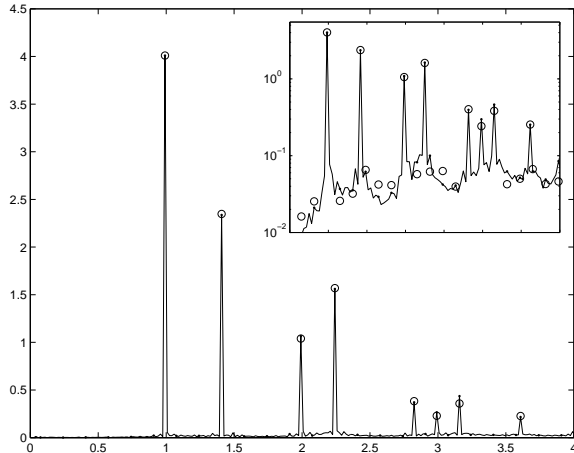


FIG. 3: Comparison of structure factor for MD (line and dots) and PFC (circles). For clarity only some of the data points are shown for PFC. The inset shows the same data on a logarithmic scale.

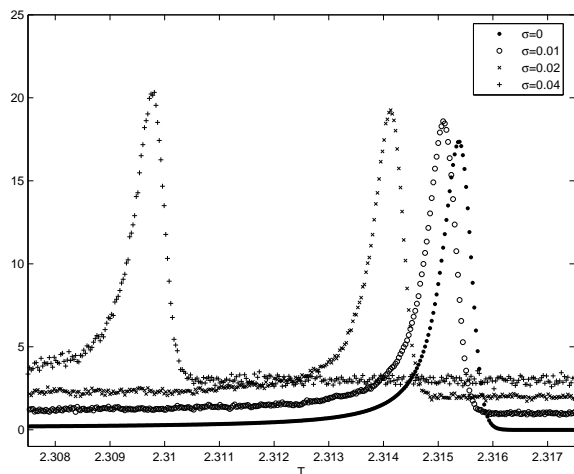


FIG. 4: Plot of $-\partial\bar{\rho}/\partial T$ as a function of T for the PFC system, where $\bar{\rho}$ is mean density and T is temperature. Results are shown for four different values of the noise strength σ . Plots are offset vertically from zero for clarity.

do not exhibit a two stage melting process.

This work was supported by the National Science and Engineering Research Council and le Fonds québécois de la recherche sur la nature et les technologies. The authors thank Ken Elder, Sami Majineni, and Dan Vernon for helpful discussions.

-
- [1] K. R. Elder, M. Katakowski, M. Haataja, and M. Grant, *Phys. Rev. Lett.* **88**, 262245701 (2002).
 - [2] K. R. Elder and M. Grant, *Phys. Rev. E* **70**, 031609 (2004).
 - [3] J. Berry, M. Grant, and K. R. Elder, *Phys. Rev. E* **73**, 031609 (2006).
 - [4] T. A. Weber and F. H. Stillinger, *Phys. Rev. E* **48**, 4351 (1993).
 - [5] A. J. Archer and M. Rauscher, *J. Phys. A: Math. Gen.* **37**, 9325 (2004).
 - [6] T. V. Ramakrishnan and M. Yussouff, *Phys. Rev. B* **19**, 2775 (1979).
 - [7] A. D. J. Haymet and D. W. Oxtoby, *J. Chem. Phys.* **74**, 2559 (1981).
 - [8] Y. Singh, *Phys. Rep.* **207**, 351 (1991).